Journal of Membrane Science Letters 5 (2025) 100109

Contents lists available at ScienceDirect

Journal of Membrane Science Letters

journal homepage: www.elsevier.com/locate/memlet

Pressure-drop reduction by oil-infused spacers

Arthur Boyko, Alina Lemster, Guy. Z Ramon *

Department of Civil & Environmental Engineering, Technion – Israel Institute of Technology, Haifa 32000, Israel

ARTICLE INFO

Keywords:
Oil infused surface
CFD
Feed spacer
Spiral-wound membrane
Pressure drop

ABSTRACT

This study explores oil-infused polydimethylsiloxane (iPDMS) feed spacers designed to reduce pressure drop in spiral-wound membrane (SWM) modules. While crucial for structural support and fouling mitigation, conventional feed spacers increase pressure drop, leading to higher energy demands. By infusing PDMS spacers with silicone oils of varying viscosities (10, 20, and 100 cSt), we achieved significant reductions in pressure drop—up to 46% compared to non-infused spacers. Lower-viscosity oils demonstrated the most pronounced improvements. Numerical simulations corroborate the experimental data, showing that the slippery surface of the oil-infused spacers minimizes flow resistance and reduces energy dissipation. These findings suggest that incorporating oil-infused spacers can enhance SWM module efficiency, offering a promising approach to lowering operational energy costs in membrane-based water treatment systems.

1. Introduction

Feed spacers are an integral component of spiral-wound membrane modules (SWM), primarily meant for providing structural support to the membrane sheets, while also facilitating some mixing, to minimize concentration polarization (CP) and fouling (Jeong et al., 2020), (Karabelas et al., 2014). However, feed spacers also increase the pressure drop along the feed channel (Saeed et al., 2012), primarily due to form drag by the obstruction and the directional changes of the flow (Dendukuri et al., 2005, Ranade and Kumar, 2006). High feed-channel pressure (FCP) drop leads to increased energy consumption and decreased permeate flux along an array of membrane modules (Koutsou et al., 2007, Koutsou et al., 2004, Lin et al., 2021).

In order to address the challenges of reducing FCP drop, research efforts have primarily focused on spacer design modifications. FCP drop tends to increase with the decrease in filament spacing (Cao et al., 2001, Shakaib et al., 2007), the increase in filament diameter (Da Costa et al., 1991, Schwinge et al., 2004), or the decrease of L_m/d_f, the ratio of the filament spacing L_m (center-to-center distance between adjacent filaments) to the filament diameter d_f, a key geometric parameter governing hydrodynamics in spacer-filled channels (Dendukuri et al., 2005), (Karode and Kumar, 2001), (Koutsou et al., 2007). Key parameters influencing spacer performance include spacer orientation (ladder/diamond type spacers), flow attack angle, and mesh angle (Gu et al., 2017, Liang et al., 2019, Amokrane et al., 2015, Bucs et al., 2018). The development of numerical simulation methods and the use of novel 3D-printed feed spacers have facilitated notable reduction of the FCP drop; in a proof-of-concept study, Sreedhar et al. developed a feed spacer with filaments based on triply periodic minimal surfaces, which increased the permeate flux and decreased the pressure drop inside the filtration channel (Sreedhar et al., 2018). Moreover, a 3D-printed, column-type spacer reduced the pressure drop by three times and doubled the specific water flux (Ali et al., 2019). In another study, symmetric perforated spacers were developed, and the perforation effect was shown to reduce the pressure drop while increasing the permeate flux (Kerdi et al., 2018). Novel helical design spacers were also developed to reduce the pressure drop inside the channel (Kerdi et al., 2020). These works on the spacers managed to achieve up to 61 % reduction in pressure drop.

Evidently, geometrical considerations have been at the forefront of spacer desing, providing several paths towards potential improvement. Herein, we examine a different, complementary strategy – creating a spacer with a slippery surface. Specifically, oil-infused surfaces are a type of slippery surface used for self-cleaning, anti-fouling, anti-icing, and anti-corrosion (Howell et al., 2018, Li et al., 2019, Villegas et al., 2019, Buddingh et al., 2021). The immobilized oil creates a liquid-liquid interface with the flowing, immiscible phase, instead of a solid-liquid interface. The oily surface is replenished by effusion of the oil from the substrate (Maccallum et al., 2015, Sotiri et al., 2018). Previous studies have shown the potential of such infused surfaces for drag-reducing applications in both turbulent (Rosenberg et al., 2016, Fu et al., 2017, Kim et al., 2020) and laminar (Solomon et al., 2014, Lee

* Corresponding author.
E-mail address: ramong@technion.ac.il (Guy.Z. Ramon).

https://doi.org/10.1016/j.memlet.2025.100109
Received 8 September 2025; Received in revised form 21 October 2025; Accepted 21 October 2025
Available online 22 October 2025
2772-4212/© 2025 The Authors. Published by Elsevier B.V. This is an open access article under the CC BY-NC-ND license (http://creativecommons.org/licenses/by-nc-nd/4.0/).

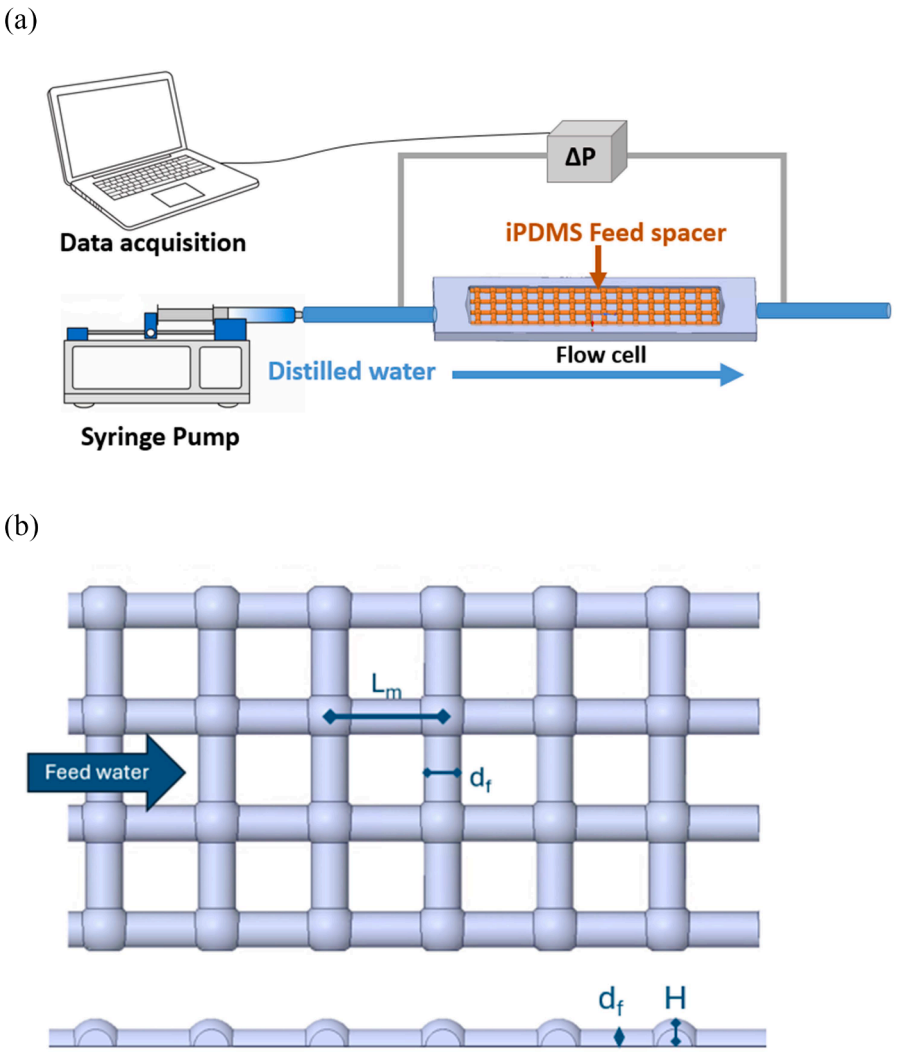


Fig. 1. (a) The experimental setup for measurement of the pressure drop over the flow cell; (b) Top-view and side view of iPDMS feed spacer presenting dimensions used.

et al., 2019, Vega-Sánchez et al., 2022) flow conditions, with decreased oil viscosity contributing to lower friction coefficients (Kant and Pitchumani, 2020). Additionally, studies have illustrated reduced adhesion and friction with decreasing viscosity of silicone oil on liquid-infused surfaces (Buene et al., 2022, Boyko et al., 2024), highlighting the potential of such surfaces in mitigating pressure drops in SWM feed channels.

In what follows, we extend the efforts outlined above to examine the impact of an oil-infused polydimethylsiloxane (PDMS)-based spacer on the feed channel pressure drop, measured at a range of Reynolds numbers for various spacer formulations. While our previous research primarily emphasized the antifouling capabilities of such spacers (Boyko et al., 2024), the present study extends the application to consider hydrodynamic aspects. Unlike previous reports, which focused on spacer geometry, the current study leverages surface engineering to achieve reduction in pressure drop, as demonstrated through experimental and computational analyses.

2. Material and methods

2.1. Fabrication of iPDMS feed spacer

The iPDMS feed spacers were fabricated using an aluminum mold, (see Fig. 1b), using PDMS (Dow Sylgard 184 polydimethylsiloxane). The polymeric base was mixed with the curing agent at a 10:1 ratio (by weight), followed by degassing under vacuum for 1 hour. The prepared PDMS was then poured into the mold and cured overnight at 60 °C. The molded PDMS was then infused at ambient temperature (25 °C) by 48 hr immersion in a bath containing silicone oil with viscosities of 10, 20 or 100 cSt (Sigma-Aldrich).

2.2. Feed spacer geometry measurement

Feed spacer dimensions were measured using a digital caliper to determine the filament spacing (mesh size) and length (L_m). The filament thickness ($d_f/2$), cross-section thickness (H channel height), and filament diameter (d_f) were precisely measured using a confocal laser scanning microscope (Leica TCS SP8) with LAS X software for 3D image acquisition and analysis, facilitated by adding a fluorescent dye to the silicone oil that was then infused into the spacer (Boyko et al., 2024). The filament thickness in our work was different from the filament diameter due to the geometric structure of the spacer. The flow cell was fabricated using a 3D printer (Bambu Lab X1 Carbon), with appropriate dimensions that ensured a fixed length and height tailored to the cross-section thickness of the spacers. The exact dimensions of the flow cell were the same as were used to fabricate the aluminum mold. The full geometric characteristics of the spacers used in this study are detailed in the supplementary information.

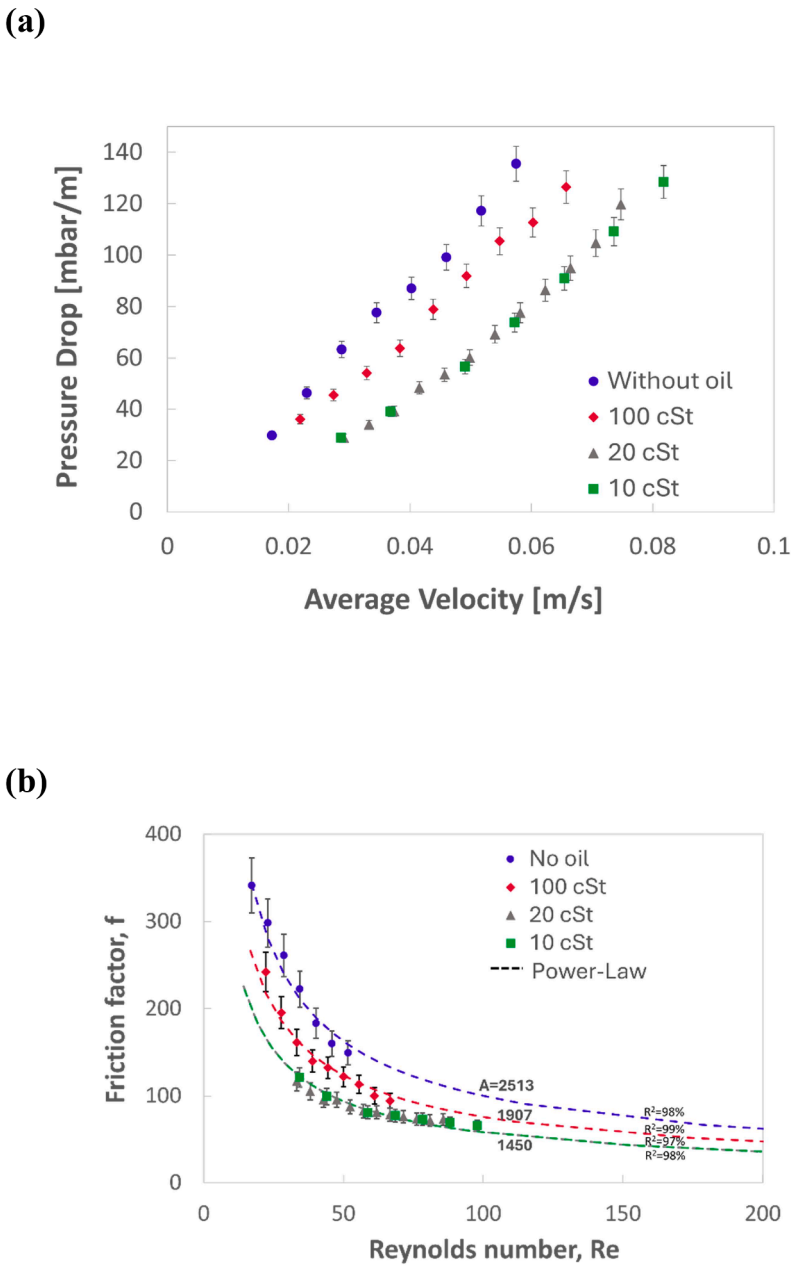


Fig. 2. (a) Measured pressure drop (mbar/m) as a function of increasing feed water average velocity (m/s). (b) The calculated friction factor plotted against the Reynolds number, including power law model (dashed lines) $f = \frac{A}{Re^n}$ with R^2 values, indicating the quality of fit between the model and experiments. The n value is 0.7. Error bars represent propagation of uncertainty. Both figures show data measured for four different PDMS feed spacers: without infused oil, and infused with 10, 20 and 100 cSt silicone oil. The data show the reduction in friction with decreasing oil viscosity within the spacer.

2.3. Experimental flow and pressure drop system

The experimental system utilized custom 3D-printed flow cells, adjusted in size for each type of spacer, namely PDMS and iPDMS with varying viscosities, as illustrated in Fig. 1. Before each experiment, the spacers were subjected to rapid agitation in water for 72 h in order to leach out any excess oil, producing a stable lubricated layer possessing the capacity for self-replenishment (Boyko et al., 2024), after which they were inserted into the flow cells. Furthermore, this pre-conditioning also aligns with standard practice and is expected to minimize interactions with detergents during any future short CIP cycles. Consistent with results reported in our previous paper (Boyko et al., 2024), extended dynamic flow experiments confirmed that oil-infused PDMS spacers retained their lubricant layer with minimal degradation under flow conditions over five days, in which the oil release reduced below detection after ~72 hrs. We note that, while long-term studies (months) are still warranted with membrane in place before actual commercial use, these results nevertheless provide confidence in the potential of the coating's robustness for typical operation. As observed in a separate study, such materials can maintain self-replenishment and durability capabilities for up to several months (Lauga et al., 2007). The dimensions of each spacer were as follows: 1) plain PDMS spacer - 11.5 mm x 58 mm x 0.8 mm, 2) iPDMS spacer infused with 100 cSt oil - 12.1 mm x 58 mm x 0.9 mm 3) iPDMS spacer infused with 20 cSt oil - 13.5 mm x 58 mm x 1 mm, and 4) iPDMS spacer infused with 10 cSt oil - 13.75 mm x 58 mm x 1.05 mm. Note that the dimensions of the spacers are slightly altered by the swelling induced by oils of varying viscosities, with lower-viscosity (10 and 20 cSt) oils causing more significant

dimensional increases (Boyko et al., 2024). These changes were accounted for by precisely matching the flow cell dimensions to each spacer type, as detailed above. Although oil swelling may introduce minor deviations in spacer geometry, the observed pressure drop reductions consistently correlate with the slippery surface properties of the oil-infused spacers, suggesting that the surface lubrication effect dominates over geometric variability. A high-precision syringe pump (PHD ULTRA, Harvard Apparatus) was used to pump deionized water into the flow cells, with a differential pressure transducer (OMEGA PX154–003DI) connected to both ends of the flow cell, measuring the pressure drop, which was recorded using LabView software. The experiments were conducted at a constant temperature of 25 °C, with varying flow rates ranging from 7 ± 0.2 to 48±1.4 mL/min, well within the operating range of the pressure transducer, ensuring accurate measurements. The range of flowrates was constrained by the measurement capacity of the sensitive differential pressure transducer (0–135 mbar/m). The flow rates for each spacer type were selected to maintain pressure drops within the transducer's reliable measurement range, while maximizing the overlap between different spacer configurations and to maintain steady, laminar conditions; results are additionally presented as friction factor vs. the Reynolds number, *Re,* to generalize beyond the specific velocities tested.

3. Numerical model

In order to gain some insight on the hydrodynamic conditions within the flow-cell, simplified numerical simulations were carried out, based on the incompressible Navier-Stokes equations,

$$\nabla\cdot\bar{v} = 0 \tag{1}$$

and

$$\rho\left(\frac{\partial\bar{v}}{\partial t} + \bar{v}(\nabla\cdot\bar{v})\right) = -\nabla p + \mu\nabla^2\bar{v}, \tag{2}$$

Where $\bar{v}$ is the velocity vector, ρ is the density, μ is the viscosity and p is the pressure.

The governing equations were solved using the software package ANSYS Fluent 2022R2, spatially discretized using a second-order upwind scheme and a coupled algorithm was used for pressure-velocity coupling. Mesh independence was verified and an absolute value of the root-mean-square residuals for velocities and mass were ensured to be below 10^{-6}, in order to provide high accuracy.

The numerical model assumes laminar flow conditions - a Reynolds number, $Re = \frac{\rho u d_h}{\mu} < 200$ (In previous work, Fimbres-Weihs and Wiley (Fimbres-Weihs and Wiley, 2010) showed that the presence of spacers in narrow channels promotes flow instabilities, but only at 200<*Re*<600). Here, d_h is the hydraulic diameter $d_h = \frac{4V}{A}$, V is fluid volume inside each cell and A is the wetted area, u is the average velocity in the cell, taken as the ratio between the volumetric flow rate Q and the empty cell cross-sectional area, multiplied by the porosity, $u = \frac{Q}{WHε}$, where W is the cell width, H is cell height, and ε is the channel porosity. Porosity, in turn, is defined as the ratio between fluid volume in the cell with spacers to empty cell (both calculated using SpaceClaim 2022R2).

The model domain corresponds, generally, with the experimental flow cell. On solid boundaries, a no-slip condition is imposed on the flow cell walls. The feed spacers, however, when infused with silicone oil, create a stable, liquid-liquid interface. The extra mobility at such an interface is approximated here as a partial slip condition - see Fig. 1a, where spacers appear in orange (see table 2 in supplementary material for boundary conditions summary). Using the Navier slip model, we have, for the velocity component tangential to the slippery surface,

$$\bar{v}_\perp = \lambda n\cdot\left[\nabla\bar{v} + (\nabla\bar{v})^T\right]\cdot(1 - nn), \tag{3}$$

in which *n* denotes the normal to the surface, directed into the liquid, and λ is referred to as the slip length (Kolle et al., 2022). The velocity component tangent to the slippery surface is required to calculate the slip velocity at each point on the surface. Since the spacer surface is curved, a local coordinate system is required for the calculation, which was implemented using UDF (user-defined function) (Sotoude et al., 2019).

The CFD analysis was not intended for experimental validation; rather, it was aimed to investigate, in a simplified manner, the underlying hydrodynamic mechanisms behind our experimental observations.

4. Results and discussion

Results indicate that the oil-infused spacers reduce the pressure drop per unit length by as much as 46 % (see Fig. 2a), achieved at an average velocity of 5–6 cm/s, which is at the lower end of typical velocities used in practice (6–20 cm/s (Vrouwenvelder et al., 2009, Horstmeyer et al., 2018)). The relative reduction is more pronounced for spacers infused with lower-viscosity oils, consistent across all tested spacers and becoming increasingly significant at higher velocities. The pressure drop measured for the non-infused and commercial spacers, is comparable with reported data (Averink, 1995, Haidari et al., 2019).

In order to eliminate geometrical effects, it is useful to recast the pressure drop data in terms of a dimensionless friction factor (Haaksman et al., 2017)

$$f = \frac{2d_h\Delta P}{Lv^2\rho}, \tag{4}$$

where *f* denotes the friction factor, Δ*P* the pressure drop *L* is a characteristic length (here taken as one element length, L_m from Fig. 1). The general trends observed for the friction factor are similar to the pressure drop, as can be expected (see Fig. 2b), the friction factor decreased notably with decreasing oil viscosity with no significant difference between viscosities of 10 cSt and 20 cSt . However, as *Re* is increased, this steep decline in the friction factor transitioned to a more gradual slope, consistent with previous observations in spacer-filled channels (Haidari et al., 2018). Reporting results as friction factor vs. Reynolds number enables interpretation beyond specific velocities, and the partial-slip model used here indicates that the relative drag-reduction trend is expected to persist at higher *Re* typical of SWM operation. The friction factors for spacers infused with 10 cSt and 20 cSt oils show negligible differences, indicating a viscosity threshold beyond which further reductions in oil viscosity does not enhance friction reduction. This can be attributed to the dynamics of the lubricant-infused layer: as oil viscosity decreases, the mobility of the oil layer increases, enhancing the slip effect at the oil-water interface. However, below a certain viscosity threshold, the slip length saturates due to the intrinsic properties of the lubricant and its interaction with the PDMS substrate, resulting in diminishing returns.

Additionally, previous stability tests (Boyko et al., 2024) demonstrated that both 10 and 20 cSt oils exhibit similar absorption and retention characteristics, with minimal oil loss under flow conditions. These findings suggest that optimizing oil viscosity should prioritize maintaining low viscosity to enhance slip, while ensuring sufficient oil retention to sustain durability over extended use.

Interestingly, the transition in the friction factor (i.e. from steep to flattened incline), observed within the range $30 < Re < 90$, may indicate a shift from steady to unsteady flow conditions, potentially accompanied by improved mixing. The pressure drop characteristics of the spacer are best expressed by a power-law correlation that relates the friction factor with the Reynolds number, written as $f = \frac{A}{Re^n}$. The constant A is a prefactor that represents the system geometry (and, hence, varied somewhat between the different spacer types). The exponent n is a reflection of the flow regime - in our experiment this was found to be a nearly constant value of 0.7 (for fully developed, laminar flow, $n = 1$). This value is also consistent with the literature for similar spacer geometries

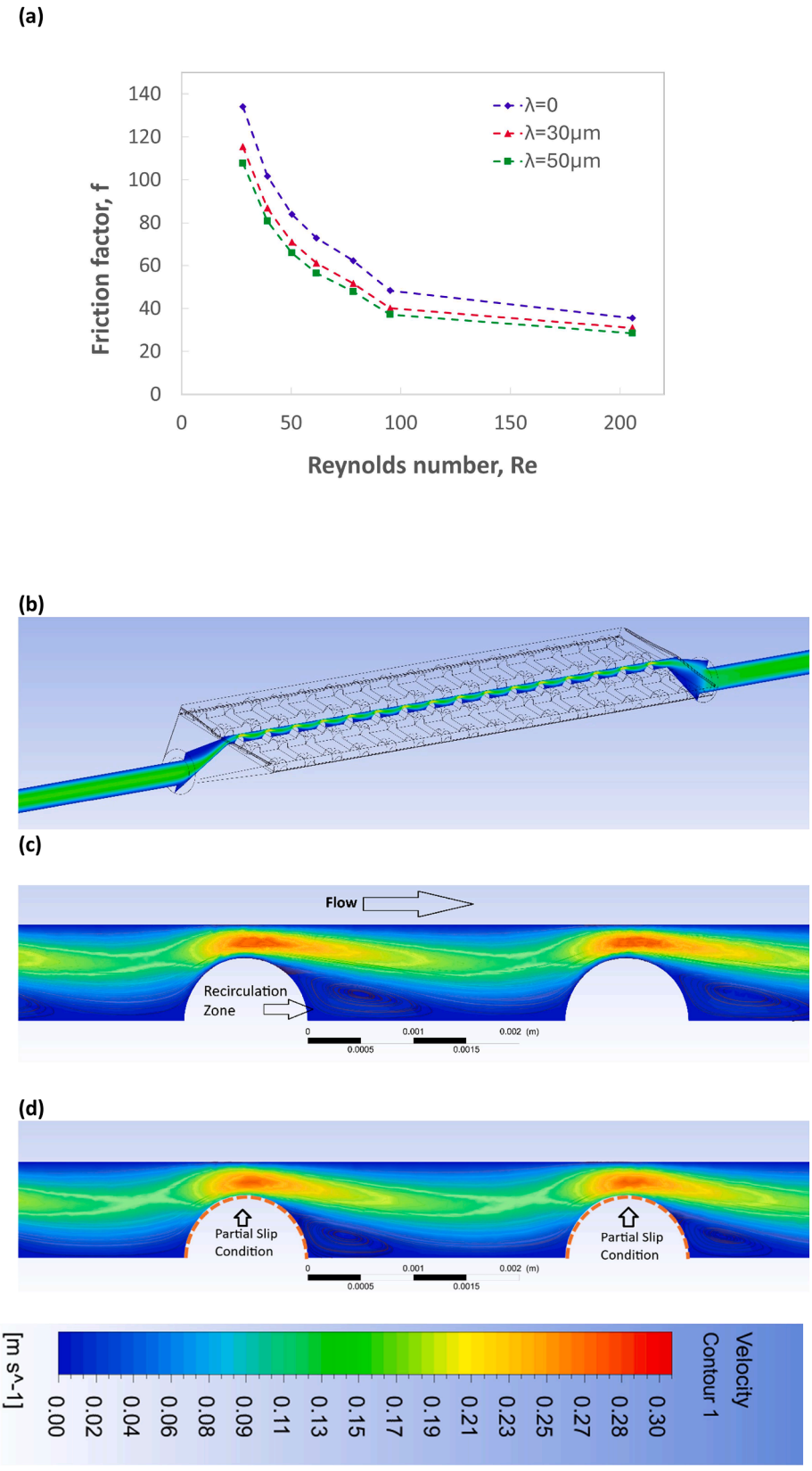


Fig. 3. (a) The calculated friction factor plotted against the Reynolds number of CFD results of cell infused with 100cSt oil for different slip boundary conditions (connecting lines are presented as visuals aids). The higher the slip length applied the lower the pressure difference across the cell. (b) Velocity contours through middle plane; (c) Zoom in to the velocity contours and pathlines at *Re*=60 of cell infused with 100cSt oil for no slip boundary condition (λ=0). (d) the partial slip boundary condition (λ=50 μm). Orange dashed lines depict filament region where partial slip condition was applied. The results show the recirculation region downstream of filaments gets smaller as slip length rises.

(Haidari et al., 2019, Han et al., 2018), indicating that the hydrodynamic regime remains relatively unchanged by the oil infusion. Further comparing our power-law fit to the literature, we note that the pre-factor (A) values, scaled by channel length, rather than a single spacer mesh length, are 144 for PDMS, 120 for iPDMS (100 cSt), and 100 for iPDMS (10, 20 cSt), slightly higher than previously reported values, e.g. Haidari (Haidari et al., 2019) provides A values ranging from 63 to 74 for ladder spacers, while Han (Han et al., 2018) reported $A = 88$ for spacers with a circular filament cross-section. This difference may likely be attributed to the specific geometry of the spacers used in this study – a simple, unoptimized geometry compared to other reported designs. However, it is important to emphasize that our primary focus is not on the geometric features themselves but rather the surface engineering, aimed to achieve hydrodynamic improvements and we anticipate that these hydrodynamic are likely transferable to other configurations. As geometric optimization falls beyond the scope of this work it represents an opportunity for future studies to yield even better results. Previous studies on spacers have managed to reduce pressure drop by 5–61 % by altering the spacer's geometry (Sreedhar et al., 2018, Ali et al., 2019, Kerdi et al., 2018, Kerdi et al., 2020). Ultimately, our oil-infused spacer was able to reduce pressure drop by up to 46 % by modifying its surface.

Contrary to previous studies, which associate a decrease in the L_m/d_f ratio with increased friction (Da Costa et al., 1994, Li et al., 2002), our study found that the highest friction coefficient corresponds to the highest L_m/d_f ratio. This suggests that the slippery surface properties introduced by oil impregnation play a critical role in reducing friction, independent of traditional geometric considerations. Additionally, the observed reduction in friction is solely attributed to decreasing oil viscosity, with no changes in hydraulic diameter (Haaksman et al., 2017).

The effect of the slippery interface on pressure drop reduction can likely be explained as an 'effective slip' of water, where the tangential velocity component is not strictly zero at the spacer surface (since it is now liquid-like). As shown in Fig. 3a, numerical calculations with a slip length of λ=50 μm resulted in a friction factor reduction of approximately 22 %, closely matching the experimental results for the 100 cSt oil-infused spacer. These simulations suggest that if indeed oil-infused surfaces induce slip, the slip length is inversely proportional to oil viscosity. The hydrodynamics within the channel reveal the expected recirculation zone behind the spacer filaments. It is apparent that the recirculation zone reduced in size when the partial slip condition was applied, as presented in Fig. 3c and d, where the velocity contours are compared with and without the slip condition. The cross-section illustrated corresponds to the mid-plane, as presented in Fig. 3b This reduction in recirculation zone size likely contributes to the overall decrease in pressure drop, as it indicates less flow disturbance and energy dissipation within the flow cell.

We note that, for practical integration, iPDMS spacers must tolerate standard CIP. After pre-conditioning (~72 h agitation), a stable, self-replenishing lubricated layer remained and was used for all measurements (Boyko et al., 2024). Within vendor CIP windows (short duration; bounded pH/temperature; low-foaming non-ionic or selected anionic surfactants; cationics discouraged), substantial lubricant loss or PDMS damage is not expected. PDMS studies report no adsorption/dissolution under short, ambient-temperature exposure to common aqueous cleaners and show hydrolytic effects mainly under extreme pH with prolonged, continuous exposure (Lee et al., 2003, Ducom et al., 2013, Khairkar et al., 2020). By analogy, the oil-in-matrix design should further limit detergent-driven depletion; future durability tests with membranes in-place are outlined (DOW FILMTEC™ Membranes, 2009, Sterlitech corporation 2015).

5. Concluding remarks

This study illustrates the potential of using oil-infused spacers to significantly reduce feed-channel pressure in SWM modules. Notably, the 10 cSt oil-infused spacer achieved a pressure drop reduction of approximately 46 % at an average velocity of 0.06 m/s, and the 20 cSt oil-infused spacer achieved similar results. The reduction in pressure drop with oil-infused spacers may be interpreted hydrodynamically in terms of a slip effect, where the slip length is inversely proportional to the oil viscosity

Integrating slippery, oil-infused surfaces into feed spacer design can potentially improve SWM module efficiency by reducing energy consumption and presents a promising direction for advancing membrane-based separation technologies.

CRediT authorship contribution statement

Arthur Boyko: Writing – review & editing, Writing – original draft, Visualization, Methodology, Investigation, Formal analysis, Data curation. **Alina Lemster:** Writing – original draft, Investigation, Formal analysis. **Guy. Z Ramon:** Writing – review & editing, Writing – original draft, Supervision, Project administration, Methodology, Funding acquisition, Formal analysis, Conceptualization.

Declaration of competing interest

The authors declare that they have no known competing financial interests or personal relationships that could have appeared to influence the work reported in this paper.

Acknowledgements

This work was funded by the Israel Science Foundation, grant #3041/21.

Supplementary materials

Supplementary material associated with this article can be found, in the online version, at doi:10.1016/j.memlet.2025.100109.

Data availability

No data was used for the research described in the article.

References

Ali, S.M., Qamar, A., Kerdi, S., Phuntsho, S., Vrouwenvelder, J.S., Ghaffour, N., Shon, H. K., 2019. Energy efficient 3D printed column type feed spacer for membrane filtration. Water Res. 164, 114961. https://doi.org/10.1016/J.WATRES.2019.114961.

Amokrane, M., Sadaoui, D., Koutsou, C.P., Karabelas, A.J., Dudeck, M., 2015. A study of flow field and concentration polarization evolution in membrane channels with two-dimensional spacers during water desalination. J. Memb. Sci. 477, 139–150. https://doi.org/10.1016/J.MEMSCI.2014.11.029.

Averink, C.A., 1995. Theorie en modellering van membraanfiltratie. H2O 302. –302.

Boyko, A., Epstein, J.A., Ramon, G.Z., 2024. Oil-infused feed spacers for biofouling inhibition. Desalination 573. https://doi.org/10.1016/j.desal.2023.117210.

Bucs, S., Farhat, N., Kruithof, J.C., Picioreanu, C., van Loosdrecht, M.C.M., Vrouwenvelder, J.S., 2018. Review on strategies for biofouling mitigation in spiral wound membrane systems. Desalination 434, 189–197. https://doi.org/10.1016/J.DESAL.2018.01.023.

Buddingh, J.V., Hozumi, A., Liu, G., 2021. Liquid and liquid-like surfaces/coatings that readily slide fluids. Prog. Polym. Sci. 123, 101468. https://doi.org/10.1016/J.PROGPOLYMSCI.2021.101468.

Buene, A.F., Auganæs, S.B., Klein-Paste, A., 2022. Effect of polydimethylsiloxane oil lubrication on the friction of cross-country UHMWPE ski bases on snow. Front. Sport. Act. Living 4. https://doi.org/10.3389/fspor.2022.894250.

Cao, Z., Wiley, D.E., Fane, A.G., 2001. CFD simulations of net-type turbulence promoters in a narrow channel. J. Memb. Sci. 185, 157–176. https://doi.org/10.1016/S0376-7388(00)00643-8.

Da Costa, A.R., Fane, A.G., Fell, C.J.D., Franken, A.C.M., 1991. Optimal channel spacer design for ultrafiltration. J. Membr. Sci. 62 (3), 275–291.

Da Costa, A.R., Fane, A.G., Wiley, D.E., 1994. Spacer characterization and pressure drop modelling in spacer-filled channels for ultrafiltration. J. Memb. Sci. 87, 79–98. https://doi.org/10.1016/0376-7388(93)E0076-P.

Dendukuri, D., Karode, S.K., Kumar, A., 2005. Flow visualization through spacer filled channels by computational fluid dynamics-II: improved feed spacer designs. J. Memb. Sci. 249, 41–49. https://doi.org/10.1016/J.MEMSCI.2004.06.062.

DOW FILMTEC™ Membranes, 2009. Cleaning Procedures for DOW FILMTEC FT30 Elements. Fact Sheet.
Ducom, G., Laubie, B., Ohannessian, A., Chottier, C., Germain, P., Chatain, V., 2013. Hydrolysis of polydimethylsiloxane fluids in controlled aqueous solutions. Water Sci. Technol. 68. https://doi.org/10.2166/wst.2013.308.
Fimbres-Weihs, G.A., Wiley, D.E., 2010. Review of 3D CFD modeling of flow and mass transfer in narrow spacer-filled channels in membrane modules. Chem. Eng. Process. Process Intensif. 49, 759–781. https://doi.org/10.1016/j.cep.2010.01.007.
Fu, M.K., Arenas, I., Leonardi, S., Hultmark, M., 2017. Liquid-infused surfaces as a passive method of turbulent drag reduction. J. Fluid. Mech. 824. https://doi.org/10.1017/jfm.2017.360.
Gu, B., Adjiman, C.S., Xu, X.Y., 2017. The effect of feed spacer geometry on membrane performance and concentration polarisation based on 3D CFD simulations. J. Memb. Sci. 527, 78–91. https://doi.org/10.1016/J.MEMSCI.2016.12.058.
Haaksman, V.A., Siddiqui, A., Schellenberg, C., Kidwell, J., Vrouwenvelder, J.S., Picioreanu, C., 2017. Characterization of feed channel spacer performance using geometries obtained by X-ray computed tomography. J. Memb. Sci. 522, 124–139. https://doi.org/10.1016/j.memsci.2016.09.005.
Haidari, A.H., Heijman, S.G.J., Uijttewaal, W.S.J., van der Meer, W.G.J., 2019. Determining effects of spacer orientations on channel hydraulic conditions using PIV. J. Water Process. Eng. 31. https://doi.org/10.1016/j.jwpe.2019.100820.
Haidari, A.H., Heijman, S.G.J., van der Meer, W.G.J., 2018. Effect of spacer configuration on hydraulic conditions using PIV. Sep. Purif. Technol. 199, 9–19. https://doi.org/10.1016/j.seppur.2018.01.022.
Han, Z., Terashima, M., Liu, B., Yasui, H., 2018. CFD investigation of the effect of the feed spacer on hydrodynamics in spiral wound membrane modules. Math. Comput. Applic. 23 (4), 80. https://doi.org/10.3390/mca23040080.
Horstmeyer, N., Lippert, T., Schön, D., Schlederer, F., Picioreanu, C., Achterhold, K., Pfeiffer, F., Drewes, J.E., 2018. CT scanning of membrane feed spacers – Impact of spacer model accuracy on hydrodynamic and solute transport modeling in membrane feed channels. J. Memb. Sci. 564. https://doi.org/10.1016/j.memsci.2018.07.006.
Howell, C., Grinthal, A., Sunny, S., Aizenberg, M., Aizenberg, J., 2018. Designing liquid-infused surfaces for medical applications: a review. Adv. Mater. 30. https://doi.org/10.1002/adma.201802724.
Jeong, K., Park, M., Oh, S., Kim, J.H., 2020. Impacts of flow channel geometry, hydrodynamic and membrane properties on osmotic backwash of RO membranes—CFD modeling and simulation. Desalination 476, 114229. https://doi.org/10.1016/J.DESAL.2019.114229.
Kant, K., Pitchumani, R., 2020. Laminar Drag Reduction in Microchannels with Liquid Infused Textured Surfaces. https://www.elsevier.com/open-access/userlicense/1.0/.
Karabelas, A.J., Koutsou, C.P., Kostoglou, M., 2014. The effect of spiral wound membrane element design characteristics on its performance in steady state desalination — A parametric study. Desalination 332, 76–90. https://doi.org/10.1016/J.DESAL.2013.10.027.
Karode, S.K., Kumar, A., 2001. Flow visualization through spacer filled channels by computational fluid dynamics I.: pressure drop and shear rate calculations for flat sheet geometry. J. Memb. Sci. 193, 69–84. https://doi.org/10.1016/S0376-7388(01)00494-X.
Kerdi, S., Qamar, A., Alpatova, A., Vrouwenvelder, J.S., Ghaffour, N., 2020. Membrane filtration performance enhancement and biofouling mitigation using symmetric spacers with helical filaments. Desalination 484, 114454. https://doi.org/10.1016/J.DESAL.2020.114454.
Kerdi, S., Qamar, A., Vrouwenvelder, J.S., Ghaffour, N., 2018. Fouling resilient perforated feed spacers for membrane filtration. Water Res. 140, 211–219. https://doi.org/10.1016/J.WATRES.2018.04.049.
Khairkar, S.R., Pansare, A.V., Shedge, A.A., Chhatre, S.Y., Suresh, A.K., Chakrabarti, S., Patil, V.R., Nagarkar, A.A., 2020. Hydrophobic interpenetrating polyamide-PDMS membranes for desalination, pesticides removal and enhanced chlorine tolerance. Chemosphere 258. https://doi.org/10.1016/j.chemosphere.2020.127179.
Kim, S.J., Kim, H.N., Lee, S.J., Sung, H.J., 2020. A lubricant-infused slip surface for drag reduction. Phys. Fluid. 32. https://doi.org/10.1063/5.0018460.
Kolle, S., Ahanotu, O., Meeks, A., Stafslien, S., Kreder, M., Vanderwal, L., Cohen, L., Waltz, G., Lim, C.S., Slocum, D., Greene, E.M., Hunsucker, K., Swain, G., Wendt, D., Teo, S.L.M., Aizenberg, J., 2022. On the mechanism of marine fouling-prevention performance of oil-containing silicone elastomers. Sci. Rep. 12. https://doi.org/10.1038/s41598-022-15553-4.
Koutsou, C.P., Yiantsios, S.G., Karabelas, A.J., 2004. Numerical simulation of the flow in a plane-channel containing a periodic array of cylindrical turbulence promoters. J. Memb. Sci. 231, 81–90. https://doi.org/10.1016/J.MEMSCI.2003.11.005.
Koutsou, C.P., Yiantsios, S.G., Karabelas, A.J., 2007. Direct numerical simulation of flow in spacer-filled channels: effect of spacer geometrical characteristics. J. Memb. Sci. 291, 53–69. https://doi.org/10.1016/J.MEMSCI.2006.12.032.
Lauga, E., Brenner, M., Stone, H., 2007. Microfluidics: the no-slip boundary condition. In: Tropea, C., Yarin, A.L., Foss, J.F. (Eds.), Springer Handbook of Experimental Fluid Mechanics. Springer Handbooks. Springer, Berlin, Heidelberg.
Lee, J.N., Park, C., Whitesides, G.M., 2003. Solvent compatibility of poly (dimethylsiloxane)-based microfluidic devices. Anal. Chem. 75. https://doi.org/10.1021/ac0346712.
Lee, S.J., Kim, H.N., Choi, W., Yoon, G.Y., Seo, E., 2019. A nature-inspired lubricant-infused surface for sustainable drag reduction. Soft. Matter. 15. https://doi.org/10.1039/c9sm01576k.
Li, F., Meindersma, G.W., De Haan, A.B., Reith, T., 2002. Optimization of non-woven spacers by CFD and validation by experiments. Desalination 146. https://doi.org/10.1016/S0011-9164(02)00472-1.
Li, J., Ueda, E., Paulssen, D., Levkin, P.A., 2019. Slippery lubricant-infused surfaces: properties and emerging applications. Adv. Funct. Mater. 29. https://doi.org/10.1002/adfm.201802317.
Liang, Y.Y., Toh, K.Y., Fimbres Weihs, G.A., 2019. 3D CFD study of the effect of multi-layer spacers on membrane performance under steady flow. J. Memb. Sci. 580, 256–267. https://doi.org/10.1016/J.MEMSCI.2019.02.015.
Lin, W., Zhang, Y., Li, D., mao Wang, X., Huang, X., 2021. Roles and performance enhancement of feed spacer in spiral wound membrane modules for water treatment: a 20-year review on research evolvement. Water. Res. 198. https://doi.org/10.1016/j.watres.2021.117146.
Maccallum, N., Howell, C., Kim, P., Sun, D., Friedlander, R., Ranisau, J., Ahanotu, O., Lin, J.J., Vena, A., Hatton, B., Wong, T.S., Aizenberg, J., 2015. Liquid-infused silicone as a biofouling-free medical material. ACS Biomater. Sci. Eng. 1, 43–51. https://doi.org/10.1021/ab5000578.
Ranade, V.V., Kumar, A., 2006. Fluid dynamics of spacer filled rectangular and curvilinear channels. J. Memb. Sci. 271, 1–15. https://doi.org/10.1016/J.MEMSCI.2005.07.013.
Rosenberg, B.J., Van Buren, T., Fu, M.K., Smits, A.J., 2016. Turbulent drag reduction over air- and liquid- impregnated surfaces. Phys. Fluid. 28. https://doi.org/10.1063/1.4939272.
Saeed, A., Vuthaluru, R., Yang, Y., Vuthaluru, H.B., 2012. Effect of feed spacer arrangement on flow dynamics through spacer filled membranes. Desalination 285, 163–169. https://doi.org/10.1016/J.DESAL.2011.09.050.
Schwinge, J., Wiley, D.E., Fane, A.G., 2004. Novel spacer design improves observed flux. J. Memb. Sci. 229, 53–61. https://doi.org/10.1016/J.MEMSCI.2003.09.015.
Shakaib, M., Hasani, S.M.F., Mahmood, M., 2007. Study on the effects of spacer geometry in membrane feed channels using three-dimensional computational flow modeling. J. Memb. Sci. 297, 74–89. https://doi.org/10.1016/J.MEMSCI.2007.03.010.
Solomon, B.R., Khalil, K.S., Varanasi, K.K., 2014. Drag reduction using lubricant-impregnated surfaces in viscous laminar flow. Langmuir 30. https://doi.org/10.1021/la5021143.
Sotiri, I., Tajik, A., Lai, Y., Zhang, C.T., Kovalenko, Y., Nemr, C.R., Ledoux, H., Alvarenga, J., Johnson, E., Patanwala, H.S., Timonen, J.V.I., Hu, Y., Aizenberg, J., Howell, C., 2018. Tunability of liquid-infused silicone materials for biointerfaces. Biointerphases 13. https://doi.org/10.1116/1.5039514.
Sotoude, H., Mirghavami, S.M., Ghorani, M.M., Riasi, A., Chini, F., 2019. A numerical study on the performance of a superhydrophobic coated very low head (VLH) axial hydraulic turbine using entropy generation method. Renew. Energy 147. https://doi.org/10.1016/j.renene.2019.09.003.
Sreedhar, N., Thomas, N., Al-Ketan, O., Rowshan, R., Hernandez, H., Abu Al-Rub, R.K., Arafat, H.A., 2018. 3D printed feed spacers based on triply periodic minimal surfaces for flux enhancement and biofouling mitigation in RO and UF. Desalination 425, 12–21. https://doi.org/10.1016/J.DESAL.2017.10.010.
Sterlitech corporation, RO /NF Cleaning Guidelines: sterlitech Membranes Cleaning Procedures for, Product Information, (2015).
Vega-Sánchez, C., Peppou-Chapman, S., Zhu, L., Neto, C., 2022. Nanobubbles explain the large slip observed on lubricant-infused surfaces. Nat. Commun. 13. https://doi.org/10.1038/s41467-022-28016-1.
Villegas, M., Zhang, Y., Abu Jarad, N., Soleymani, L., Didar, T.F., 2019. Liquid-infused surfaces: a review of theory, design, and applications. ACS Nano 13. https://doi.org/10.1021/acsnano.9b04129.
Vrouwenvelder, J.S., Hinrichs, C., van der Meer, W.G.J., van Loosdrecht, M.C.M., Kruithof, J.C., 2009. Pressure drop increase by biofilm accumulation in spiral wound RO and NF membrane systems: role of substrate concentration, flow velocity, substrate load and flow direction. Biofouling 25. https://doi.org/10.1080/08927010902972225.